

Nucleation and growth in the initial stage of metastable titanium disilicide formation

Z. Ma, Y. Xu, and L. H. Allen

Department of Materials Science and Engineering and Coordinated Science Laboratory, University of Illinois, Urbana, Illinois 61801

S. Lee

Microelectronics Division, NCR Corporation, Colorado Springs, Colorado 80916

(Received 27 January 1993; accepted for publication 4 May 1993)

Initial stage of the C49-TiSi₂ formation was investigated at 530 °C and at a rate of 10 °C/m using transmission electron microscopy. Morphological studies reveal that the C49 phase first separately nucleates at the interface between amorphous silicide and crystalline silicon, then followed by simultaneous lateral and vertical growth. The growth proceeds very fast until the formation of a continuous layer of C49-TiSi₂. Local chemical analysis shows that the composition range of the amorphous silicide is narrowed due to the C49 formation. For isothermal annealing, a linear density of the C49 nuclei is about $6.7 \times 10^{-3}/\text{\AA}$, and remains the same upon prolonged annealing. In the case of annealing at 10 °C/m, the linear density depends on temperature, reaching a maximum of $7.2 \times 10^{-3}/\text{\AA}$ at around 575 °C.

The formation of titanium disilicides through the reaction of titanium with crystalline silicon has been extensively studied from different aspects because of their important technological applications in integrated circuits.^{1,2} It has been consistently reported that after an amorphous silicide formation, a high-resistivity metastable titanium disilicide (C49 structure) always forms before a low-resistivity stable titanium disilicide (C54 structure), and is inevitable during conventional furnace annealing³⁻⁵ as well as rapid thermal annealing.⁶ To form reliable shallow junctions and smooth interfaces, one desires an understanding of the reaction kinetics of both disilicides. Unfortunately, previous reports on the reaction rates of Ti with *c*-Si are far from consistent.⁷⁻¹⁰ Hung *et al.*⁷ showed difficulties in reproducing the kinetics of C49 phase formation, and attributed this lack of reproducibility to the presence of impurities at the interface. Recently, Raaijmakers *et al.*⁸ have indicated that for the C49 phase formation, the reaction proceeds much faster in the initial stage before the diffusion-controlled stage of the reaction sets in. They found that the irreproducibility was observed in the initial stages of the C49 formation, and was not due to the interfacial impurities. Since their results were obtained by Rutherford backscattering spectrometry (RBS), a technique that has limited depth resolution and is relatively insensitive to the initial stage of the reaction, it appears necessary to examine this initial stage more closely in order to acquire a more detailed picture about the two distinct kinetic regimes of the C49 phase formation.

In this Communication, we report our studies on the initial stages of the C49 phase formation under the conditions of isothermal and constant-heating-rate annealing using cross-sectional transmission electron microscopy (XTEM) coupled with a scanning transmission electron microscope (STEM) probe. Our results clearly delineate the initial stage of the C49 formation. Morphological evolution is explained by considering both local chemistry and

kinetic feasibility. This initial fast evolving stage is also discussed on the basis of the competition between nucleation and growth of the C49 phase.

p-type Si (100) wafers with a 750-nm-thick thermal oxide were employed in this study. After degreasing, a 350 nm phosphorus doped polycrystalline Si film was first grown onto the oxidized Si wafers using low-pressure chemical vapor deposition (LPCVD). A Ti film of 55 nm in thickness was then deposited over the polycrystalline Si using rf sputtering. Isothermal annealing and constant-heating-rate annealing were carried out in high vacuum (10^{-7} Torr) at 530 °C for various times and at 10 °C/m, respectively. Details of the experiment are discussed elsewhere.⁴ Growth morphology of the C49-TiSi₂ phase was characterized using XTEM. Local chemical analysis was performed using a VG HB5 STEM with a 10 Å probe. The phase identification of the C49 phase was carried out using the TEM microdiffraction technique.

Both isothermal annealing and constant-heating-rate annealing resulted in quite similar morphological development, as revealed by XTEM examinations. For the sake of clarity, we only show the results for samples annealed at a heating rate of 10 °C/m. Figure 1(a) shows a micrograph for a sample heated up to about 510 °C. It is clearly seen that a metastable C49-TiSi₂ phase individually nucleated along the interphase boundary between amorphous silicide (*a*-TiSi_{*x*}) and crystalline Si (*c*-Si). This is consistent with previous observations,^{3,4} see Ref. 11. The shape of the nuclei is typical of heterogeneous nucleation, and is featured by the curvature toward the *c*-Si being larger than that toward the *a*-TiSi_{*x*}, implying that interfacial energy on the *a*-TiSi_{*x*} side is larger than on the *c*-Si side.¹² The same features were also seen from a sample annealed at 530 °C for 13 min.

Upon annealing to a higher temperature or at 530 °C for a longer time, the C49-TiSi₂ grains grew laterally (in a direction parallel to the *a*-TiSi_{*x*}/*c*-Si interface), as well as

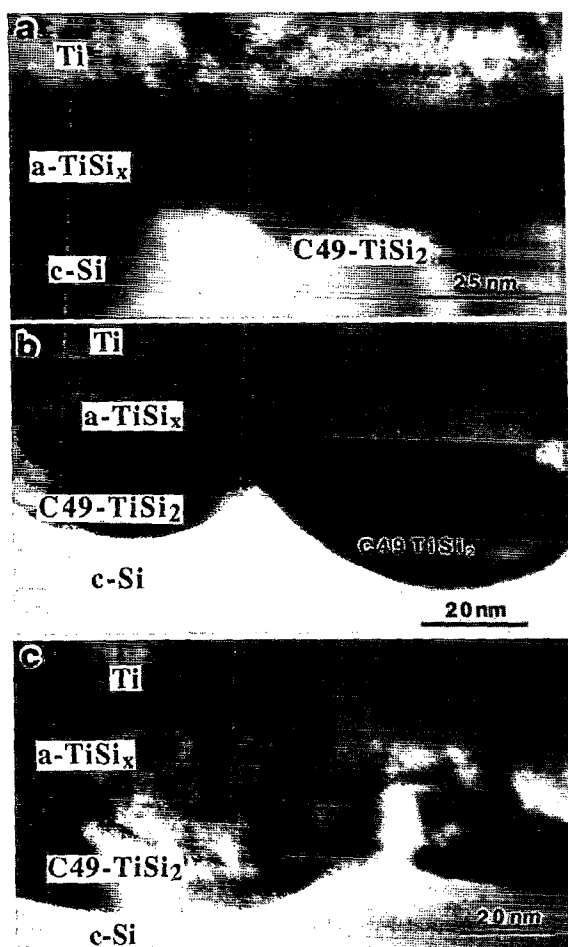


FIG. 1. XTEM micrographs for samples annealed at $10^\circ\text{C}/\text{m}$ up to (a) $\sim 310^\circ\text{C}$; (b) $\sim 560^\circ\text{C}$, and (c) $\sim 585^\circ\text{C}$.

vertically (in a direction perpendicular to the interface) at the expense of $a\text{-TiSi}_x$ and Si. The lateral growth (lengthening) appears faster than the vertical growth (thickening). The vertical growth is characterized by the further protrusion of the $\text{C49-TiSi}_2/c\text{-Si}$ boundary into the $c\text{-Si}$, thus giving rise to the rough interface, but the growth at the $a\text{-TiSi}_x/\text{C49-TiSi}_2$ interface seems very slow [Fig. 1(b)]. Further simultaneous lateral and vertical growth resulted in the coalescence of the individual grains originally separately formed at the interface. This initial growth stage proceeds very fast, as illustrated in Fig. 1(b) for a sample annealed up to $\sim 560^\circ\text{C}$. The stacking faults are revealed by the (020) lattice fringes in larger C49-TiSi_2 grains, as typically observed along this stacking sequence in the C49 phase.¹³ Figure 1(c) shows an XTEM micrograph obtained from a sample heated to $\sim 585^\circ\text{C}$. As seen from the figure, finally, the individual growing C49-TiSi_2 grains connected each other to form a continuous layer of polycrystalline C49-TiSi_2 before the Ti film and $a\text{-TiSi}_x$ phase are exhausted. It is also worth noting that in either case, a continuous layer of C49 phase is formed from a relatively few large C49 nuclei, thus resulting in very large C49 grains [see Fig. 1(c)]. At this stage, the simultaneous

growth behavior of the C49 phase changed over to mainly vertical growth.

In both annealing cases, a linear density of the C49 nuclei was measured along the interface based upon a number of XTEM micrographs made for each sample. Our preliminary results indicate that for isothermal annealing at 530°C for about 15 min, the linear density is about $6.7 \times 10^{-3}/\text{\AA}$ and remains almost the same during prolonged annealing. But in the case of annealing at $10^\circ\text{C}/\text{m}$, the linear density initially depends upon temperature, increasing from $3.2 \times 10^{-3}/\text{\AA}$ ($\sim 520^\circ\text{C}$) to $7.2 \times 10^{-3}/\text{\AA}$ ($\sim 570^\circ\text{C}$). The relative large increase is observed at about $535\text{--}540^\circ\text{C}$ ($6.0 \times 10^{-3}/\text{\AA}$).

To understand the morphological evolution described above, we also performed a local chemical analysis along several interphase boundaries, i.e., $\text{Ti}/a\text{-TiSi}_x$, $a\text{-TiSi}_x/c\text{-Si}$, and $a\text{-TiSi}_x/\text{C49-TiSi}_2$. Figure 2(a) shows approximate locations of the STEM probe during analysis. The effective probe size was estimated to be $\sim 40 \text{\AA}$, based upon the possible drifting of the specimen and beam broadening effect. The compositions measured for the C49 phase were also included for comparison. These results are summarized in Fig. 2(b). It reveals two important facts: (1) the $a\text{-TiSi}_x$ layer has a composition range from ~ 33 at. % Si (at the $\text{Ti}/a\text{-TiSi}_x$ interface) to ~ 67 at. % Si (at the $a\text{-TiSi}_x/c\text{-Si}$ interface), similar to the results reported by Ogawa *et al.*,¹⁴ and (2) due to the formation of the C49 phase the composition range for the $a\text{-TiSi}_x$ layer is narrowed, changing from ~ 67 at. % Si ($a\text{-TiSi}_x/c\text{-Si}$) to ~ 52 at. % Si ($a\text{-TiSi}_x/\text{C49-TiSi}_2$). This can also be explained qualitatively using a schematic Gibbs free energy versus composition diagram shown in Fig. 3. Thus, the results should be qualitatively quite general though the actual local compositions are temperature dependent.

As pointed out by Raaijmakers *et al.*,⁸ the kinetics of the C49 formation can be described as two regimes: initial fast reaction and diffusion-controlled growth, being represented by different kinetic rates. From this study, we have shown that the initial stage of the reaction is essentially associated with the discontinuous nucleation of the C49 phase, then followed by the simultaneous lengthening and thickening. The simultaneous growth exhibits a large disparity in growth rates of the C49 grains in vertical and lateral directions. This initial growth stage proceeds very fast until a continuous layer of C49 phase forms. The disparity in the growth rates can be easily understood based on the local chemical information. Before the C49 phase forms, the $a\text{-TiSi}_x$ layer has a larger composition range across the entire layer. The composition at the $a\text{-TiSi}_x/c\text{-Si}$ interface is about 33 at. % Ti and 67 at. % Si, very close to the composition required for the C49 formation.¹⁴ After the formation of the C49 phase, the composition shifts from ~ 67 at. % Si to ~ 52 at. % Si at the $a\text{-TiSi}_x/\text{C49-TiSi}_2$ interface. Such a composition barrier slows down the vertical growth at this interface, since a further growth would require more Si supply either through the already existing C49 phase (lattice diffusion) or along the interphase boundaries (interphase boundary diffusion) to the growth front. This explains the slow

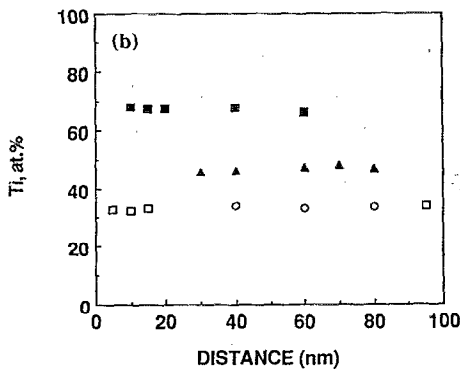
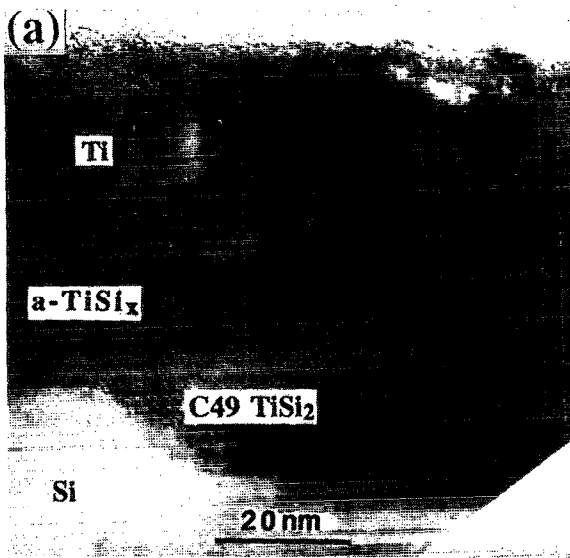


FIG. 2. (a) An XTEM micrograph for a sample annealed at 530 °C for 15 min, showing approximate locations of the STEM nanoprobe during analysis; (b) local compositions at different interphase boundaries measured by STEM (□= $a\text{-TiSi}_x/\text{Si}$ interface; ▲= $a\text{-TiSi}_x/\text{C49-TiSi}_2$ interface; ■= $\text{Ti}/a\text{-TiSi}_x$ interface, ○= C49-TiSi_2).

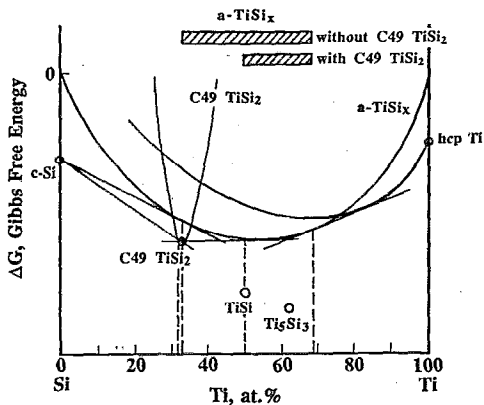


FIG. 3. Schematic Gibbs free energy vs composition diagram for the Ti-Si binary system, showing the local equilibria established by the common tangents among different phases.

growth observed at this interface. Instead, the lateral growth can be facilitated by the local transport of Si along the $\text{C49-TiSi}_2/c\text{-Si}$ interface to the growth front. This point is supported by the known fact that Si is the dominant moving species in the C49 phase growth.¹⁵ Also from the observed simultaneous growth behavior, we suggest that the initial fast growth is dominated by the preferential diffusion of Si along the interphase boundaries to the growth front rather than through the existing C49 phase. The lattice diffusion is expected to be operative in the later stage of the growth, so as to give a slow reaction rate.⁸

The reason for the lack of control of the initial C49 phase formation is still not quite clear at present. It is mostly likely related to the nucleation difficulties of the disilicide on $c\text{-Si}$. As indicated by d'Heurle,¹² nucleation of C49-TiSi_2 at the $a\text{-TiSi}_x/c\text{-Si}$ interface is driven by a very small negative free energy change. So it can be very sensitive to temperature, stress, and the presence of heterogeneous nucleation sites. Our number density data suggest that there exists a threshold temperature (around 530 °C) for the nucleation of the C49 phase. At a temperature close to the threshold temperature, once the C49 phase is successfully nucleated, the next step is more likely associated with the growth of the present nuclei rather than further nucleation, even though such nucleation sites may still exist. As the temperature is far above the critical temperature, all the nucleation sites are expected to be filled within a very short time, a well-defined diffusion-controlled growth regime will quickly take over the initial growth stage of the C49 phase. Therefore, to be more precise, we think that the initial stage of the C49 phase formation may represent the competition between the nucleation and growth of the disilicide.

This work is partially supported by the Joint Services Electronics Program (JSEP) under Contract No. N00014-90-J-1270 (A. Goodman).

- ¹R. Beyers and R. Sinclair, *J. Appl. Phys.* **57**, 5240 (1985).
- ²R. Beyers, D. Coulman, and P. Merchant, *J. Appl. Phys.* **61**, 5110 (1987).
- ³A. Kirtikar and R. Sinclair, *Mater. Res. Soc. Symp. Proc.* **260**, 227 (1992).
- ⁴Z. Ma, L. H. Allen, and S. Lee, *Mater. Res. Soc. Symp. Proc.* **237**, 661 (1992).
- ⁵R. D. Thompson, H. Takai, P. A. Psaras, and K. N. Tu, *J. Appl. Phys.* **61**, 540 (1987).
- ⁶L. A. Clevenger, J. M. E. Harper, C. Cabral, Jr., C. Nobilli, G. Ottaviani, and R. Mann, *J. Appl. Phys.* **72**, 4978 (1992).
- ⁷L. S. Hung, J. Gyulai, J. W. Mayer, S. S. Lau, and M. A. Nicolet, *J. Appl. Phys.* **54**, 5076 (1983).
- ⁸I. J. M. M. Raaijmakers, L. J. V. IJzendoorn, A. M. L. Theunissen, and K. B. Kim, *Mater. Res. Soc. Symp. Proc.* **146**, 267 (1989).
- ⁹C. A. Pico and M. G. Lagally, *J. Appl. Phys.* **64**, 4957 (1988).
- ¹⁰S. S. Iyer, C. Y. Ting, and P. M. Fryer, *J. Electrochem. Soc.* **132**, 2240 (1985).
- ¹¹Very occasionally, TiSi is detected, but its further growth is not seen.
- ¹²F. M. d'Heurle, *J. Mater. Res.* **3**, 167 (1988).
- ¹³T. C. Chou, C. Y. Wong, and K. N. Tu, *J. Appl. Phys.* **62**, 2275 (1987).
- ¹⁴S. Ogawa, T. Kouzaki, T. Yoshida, and R. Sinclair, *J. Appl. Phys.* **70**, 827 (1991).
- ¹⁵W. K. Chu, S. S. Lau, J. W. Mayer, H. Muller, and K. N. Tu, *Thin Solid Films* **25**, 393 (1975).